

Introduction

A critical observation dating back to the early days of functional neuroimaging is that a distributed network of brain regions is frequently active across a variety of cognitive challenges. This so-called task-positive network (alternatively, multiple-demand network) is thought to be underlie effortful, goal-directed cognition across a wide variety of psychological domains. Moreover, extensive evidence from neuropsychology, primate electrophysiology and fMRI has suggested that lateral portions of the frontal lobe are particularly critical for the execution of flexible behavior under a wide variety of task-demands. However, the precise correspondence of computational processes to distinct anatomical sub-regions across this vast network, and specifically lateral frontal cortex, is highly debated.

There have been several attempts to better understand the organization of regions that compose this network on the basis of its architectonic properties {Petrides:2005hc} (Figure 1A) and in-vivo measurements of structural and resting-state functional connectivity MRI (rs-fcMRI). Notably, graph theoretic approaches applied to rs-fc MRI have more precisely characterized the dynamics of the different constituents of this network, and suggested the existence at least two distinct control sub-networks: the fronto-parietal network (FPN) and cingulo-opercular network (CON) (Figure 1B). However, although these studies have greatly advanced our understanding of the organization of task-positive regions such methods cannot directly demonstrate the functional significance of the resulting regions as they do not measure their response to various psychological challenges.

To this end, functional MRI (fMRI) has been extensively used to associate distinct foci of the task-positive network—and in particular regions in frontal cortex—with activation across a wide

variety of psychological challenges designed to differ in their demands for control. In turn, these associations have led to detailed, but sometimes conflicting, theories of how information processing in task-positive regions results in flexible, adaptive behavior. For example, activity in left DLPFC has been associated with the resolution of non-response conflict {Milham:2001ef}, the retention of information in working-memory and the maintenance of task-goals in the face of distractors. Others have suggested a rostro-caudal hierarchical axis of cognitive control along lateral prefrontal cortex, citing evidence that posterior LFC is more active for low-level motoric demands whereas fronto-polar regions are active for high-level abstract planning. Additionally, some cite the robust activation of posterior LPFC, in a region named the inferior frontal junction (IFJ), to suggest that IFJ is critical for set-shifting.

Despite the enormous amount of neuroimaging studies, there have been few large-scale efforts to comprehensively map the full range of psychological functions, including dissociable aspects of cognitive control, onto the task-positive networks. Because most researchers tend to be intimately familiar with a particular psychological domain, most meta-analyses are restricted to a relatively small subset of empirical findings or a small region of interest (e.g. set-switching in IFJ {Derrfuss:2005bh}). This narrow scope necessarily limits the ability to address the specificity of activation of psychological states across task-positive network anatomy. That is, without considering a wide representative range of psychological states, it is difficult to determine whether particular kinds of tasks preferentially recruit specific regions of the task-positive network. This limitation, widely known as the reverse inference problem (Poldrack, 2006), is particularly acute in regions of the brain that show a high rate of activation across tasks, raising questions about their whether these regions are selectively involved in specific mental functions (Nelson et al., 2010a; Yarkoni et al., 2011). Thus, by the very nature of the task-

positive network being involved in many tasks across wide variety of psychological domains, this network is particularly difficult to associate to specific mental operations (Figure 1C).

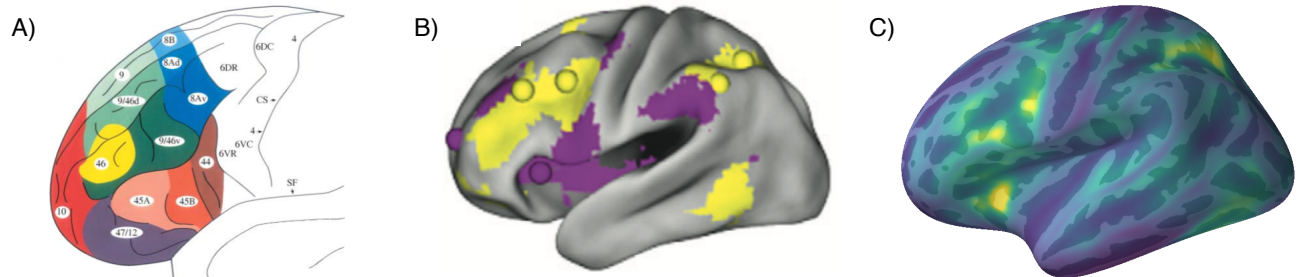


Figure 1. A) Cyto-architectonic parcellation of human lateral frontal cortex based on Petrides and Pandya (1996). B) Control networks of the human brain derived using graph theory in rs-fc MRI based on Power et al., (2012). Frontoparietal network (yellow) and cingulo-opercular network (purple). C) Base rate of activation for voxels across the brain in Neurosynth. Note that key regions of the task-positive network, such as LPFC, anterior insula and lateral parietal cortex are active in a high percentage of studies.

Here we address these issues by creating a comprehensive mapping between psychological states task-positive network anatom using Neurosynth (Yarkoni et al., 2011), a framework for large-scale fMRI meta-analysis composed of nearly 11,500 studies. First, we defined the task-positive network and clustered voxels into functionally dissociable sub-regions at several spatial scales based on their meta-analytic co-activation with the rest of the brain (Toro et al., 2008; Smith et al., 2009; Robinson et al., 2010). In contrast to cytoarchitectonic and connectivity based parcellations, the present analysis identified clusters with distinct signatures of functional activation across a wide range of psychological manipulations. In order to avoid restricting ourselves to an unnecessarily small subset of regions and to avoid defining biased or arbitrary boundaries for this network, we clustered the whole cortex to identify the task-positive network,

and subsequently parcellated this network into smaller constituents. Moreover, we largely focused on sub-regions in lateral frontal cortex, as these regions are thought to play a central role in flexible, adaptive behavior. We then characterized each cluster's psychological profiles using multivariate classification, revealing broad shifts in function between three sub-networks of the task-positive network and subtler, yet distinct, functional signatures between regions in each sub-networks. Collectively, our results provide a comprehensive functional map of the task-positive network at several anatomical scales using unbiased data-driven methods.

Materials & Methods

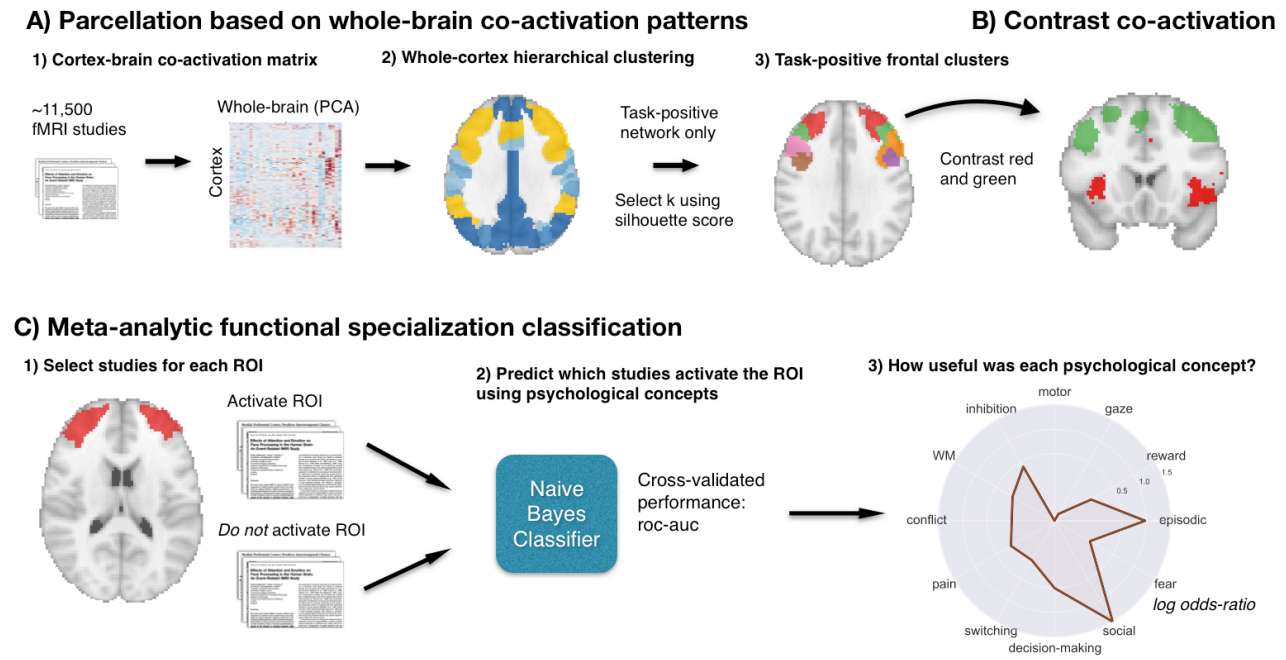


Figure 2. Methods overview. A) Whole brain co-activation of cortical voxels was calculated and hierarchical ward clustering was applied resulting in whole-brain networks. We focused only on frontal clusters within the task-positive networks and identified spatially distinct clusters B) We compared the whole-brain co-activation of pairs of clusters that were in the same branch of hierarchical clustering results C) We generated functional preference profiles for each cluster by determining which psychological topics best predicted their activation.

We analyzed version 0.6 of the Neurosynth database, (Yarkoni et al., 2011), a repository of 11,406 fMRI studies and over 410,000 activation peaks. Each observation contains the peak activations for all contrasts reported in a study's table as well as the frequency of words in the article abstract. As peak activations are populated automatically, the database does not differentiate between Talairach and MNI coordinates; however, all activations are treated as MNI coordinates, and all of the following analyses are in MNI152 coordinate space. Scikit-learn

(Pedregosa et al., 2011), a Python module, was used for all machine learning analyses. Analyses were performed using the core Neurosynth python tools.

Co-activation clustering

In order to avoid potentially biased or arbitrary boundaries, we clustered the entire cortex on the basis of meta-analytic co-activation and focused subsequent analyses on lateral frontal regions that are part of the task-positive network. We clustered individual grey matter cortical voxels based on their meta-analytic co-activation with voxels in the rest of the brain (Figure 2A). We defined a cortical mask by only including voxels with a greater than 30% probability of occurring in grey matter cortex according to the Harvard-Oxford anatomical atlas and very low activation in the database (less than 100 studies per voxel). Next, we calculated the co-activation of each cortical voxel and every other voxel in the brain (including sub-cortex). Activation for each voxel is represented as a binomial vector of length 11,406, with 1 indicating that that voxel was active in a particular study. As the cross-correlation between grey matter voxels and every other voxel in the brain resulted in a very large matrix (112,358 x 171,524) that would be computationally costly to cluster, we reduced the dimensionality of the rest of the brain from 171,524 voxels to 100 components using principal components analysis (PCA). Then, we computed the Pearson correlation distance between every voxel in the grey matter mask with each whole-brain PCA component, resulting in a 112,358 grey matter voxel x 100 whole-brain component cross-correlation matrix. We applied hierarchical clustering with ward's to this matrix, calculating a full linkage matrix. Hierarchical clustering was used as this algorithm was recommended as the best compromise between accuracy (e.g fit to data) and reproducibility for fMRI clustering (Thirion et al., 2014). However, this clustering algorithm is seldom used because the computational time increases cubically [$\Theta(N^3)$] as a function of samples. We

employed the fastcluster algorithm {Mullner:2013bl} — a package of libraries that enable efficient hierarchical clustering [$\Theta(N^3)$] — to achieve whole-brain clustering. From the whole-brain clustering, we isolated the task-positive network (consisting of lateral frontal regions, pre-SMA, the insula and lateral parietal regions) at $k = 5$; this network consisted of about 22,343 voxels and included most of the lateral frontal cortex except for most of precentral gyrus, anterior superior frontal gyrus and right lateral orbital cortex. The following analyses focus on this subset of the clustering results.

Since the optimality of a given clustering depends in large part on investigators' goals, the preferred level of analysis, and the nature and dimensionality of the available data, identifying the 'correct' number of clusters is arguably an intractable problem (Poldrack, Yarkoni, 2016). However, in the interest of pragmatism, we attempted to objectively select the number of clusters using the silhouette score, a measure of within-cluster cohesion. The silhouette coefficient was defined as $(b - a) / \max(a, b)$, where a is the mean intra-cluster distance and b is the distance between a sample and the nearest cluster that the sample is not a part of. Solutions that minimized the average distance between voxels within each cluster received a greater score. We produced flat clusters from the full hierarchical linkage matrix at 3 to 35 clusters and calculated the silhouette for each solution. We focus the following analyses on solutions that showed a local maxima at various spatial scales (i.e. 3, 9, 15 & 27 regions), but do not make a strong argument that these specific number of regions are neuroscientifically meaningful.

To understand the anatomical correspondence of the resulting clusters, we calculated the probability of voxels in each cluster of occurring in probabilistic regions from the Harvard-Oxford atlas (H-O). We refer to H-O's Juxtapositional Lobule Cortex as Supplementary Motor Area (SMA) for consistency. We also compared the location of clusters to regions from

cytoarchitectonic atlases of lateral frontal area {Petrides:2005hc}. Regions were given names based on anatomical probabilities as well as subjective preferences.

Co-activation profiles

Next, we analyzed the differences in whole brain co-activation between the resulting clusters (Figure 2B) at two spatial scales: nine and fifteen regions. To do so, we performed a meta-analytic contrast between studies that activated a given cluster, and studies that activated control clusters. The resulting images indicate voxels with a greater probability of co-activating with the cluster of interest than with control clusters. For the nine-cluster solution, we contrasted the co-activation between the four clusters primarily located in frontal cortex (i.e. LPFC/preSMA, rIFS, VRPFC, & lIFS). However, for the fifteen-cluster solution, there were too many frontal cortex regions to visualize in one image. Thus, we contrasted related sets of clusters that were leaves in the same node at the nine-cluster level, excluding clusters located outside of frontal cortex. For example, voxels in red in the first panel of Figure 7A indicate voxels that are active more frequently in studies in which RLPFC is active than in studies in which DLPFC is active; pre-SMA was excluded as it is located on the medial surface, primarily. We calculated p-values for each voxel using a two-way chi-square test and thresholded the co-activation images using False Discovery Rate ($q < 0.01$). The resulting images were binarized for display purposes and visualized using the NiLearn library for Python.

Topic modeling

Although term-based meta-analysis maps in Neurosynth closely resemble the results of manual meta-analyses of the same concepts, there is a high degree of redundancy between terms (e.g. ‘episodes’ and ‘episodic’), as well as potential ambiguity as to the meaning of an individual

word out of context (e.g. ‘memory’ can indicate working memory or episodic memory). To remedy this, we employed a reduced semantic representation of the latent conceptual structure underlying the neuroimaging literature: a set of 60 topics derived using latent dirichlet allocation (LDA) topic-modeling. This procedure was identical to that used in a previous study (Poldrack et al., 2012a), except for the use of a smaller number of topics and a much larger version of the Neurosynth database. The generative topic model derives 60 independent topics from the co-occurrence across studies of all words in the abstracts fMRI studies in the database. Each topic loads onto individual words to a varying extent, facilitating the interpretation of topics; for example, a working memory topic loads highest on the words ‘memory, WM, load’, while an episodic memory topic loads on ‘memory, retrieval, events’. Note that both topics highly load on the word “memory”, but the meaning of this word is disambiguated because it is contextualized by other words that strongly load onto that topic. Although the set of topics included around 25 topics representing non-psychological phenomena-- such as the nature of the subject population (e.g. gender, special populations) and methods (e.g., words such as “images”, “voxels”)—these topics were not excluded as they were rarely the strongest loading topics for any region. See Table 1 for a list of topics most associated with lateral frontal cortex.

Meta-analytic functional preference profiles

We generated functional preference profiles by determining which psychological topics best predicted each cluster’s activity across fMRI studies (Figure 2C). First, we selected two sets of studies: studies that activated a given cluster--defined as activating at least 5% of voxels in the cluster-- and studies that did not--defined as activating no voxels in the cluster. For each cluster, we trained a naive Bayes classifier to discriminate these two sets of studies based on psychological topics herein. We chose naive Bayes because (i) we have previously had success

applying this algorithm to Neurosynth data (Yarkoni et al., 2011); (ii) these algorithms perform well on many types of data (Androutsopoulos et al., 2000), (iii) they require almost no tuning of parameters to achieve a high level of performance; and (iv) they produce highly interpretable solutions, in contrast to many other machine learning approaches (e.g., support vector machines or decision tree forests).

We trained models to predict if fMRI studies activated each cluster, given the semantic content of the studies. In other words, if we know what psychological states are described in a study how well can we predict if it activates a specific region? We used 4-fold cross validation for testing and calculated the mean score across all folds as the final measure of performance. We scored our models using the area under the curve of the receiver operating characteristic (AUC-ROC) --a summary metric of classification performance that take into account both sensitivity and specificity. AUC-ROC was chosen this measure is not detrimentally affected by unbalanced data (Jeni et al., 2013), which was important because each region varied in the ratio of studies that activated it to the studies that did not.

To generate functional preference profiles, we extracted from the naive Bayes models the log odds-ratio (LOR) of a topic being present in active studies versus inactive studies. The odds-ratio was defined as the probability of a topic in active studies over the probability of the topic in inactive studies, for each region. LOR values above 0 indicate that a psychological topic is predictive of activation of a given region. To determine the significance of these associations, we permuted the class labels indicating if a study activated a region and extracting the LOR for each topic, 1000 times. This resulted in a null distribution of LOR for each topic and each cluster. Using this null distribution, we calculated p-values for each pairwise relationship between psychological concepts and regions, and reported associations significant after controlling for

multiple comparisons using False Discovery Rate with $q < 0.01$. Finally, to determine if certain topics showed greater preference for one cluster versus another, we conducted exploratory, post-hoc comparisons by determining if the 95% confidence intervals (CI) of the LOR of a specific topic overlapped between two regions. We generated CIs using bootstrapping, sampling with replacement and recalculating log-odds ratios for each region 1000 times.

Results

Functionally separable lateral frontal regions of the task-positive network

We identified spatially dissociable regions on the basis of shared co-activation profiles with the rest of the brain (Toro et al., 2008; Smith et al., 2009; Chang et al., 2013), an approach that exploits the likelihood of a voxel co-activating with another voxel across studies in the meta-analytic database. To avoid defining arbitrary boundaries for task-positive regions in the lateral frontal cortex, we clustered the entire cortex and identified large-scale networks at a coarse spatial scale ($k=5$). At this scale, several networks consistent with previous descriptions were present, such as the default network, visual network, dorsal attention network, auditory network, and the task-positive network (Figure 3). Having identified the task-positive network, we focused subsequent analyses on this network exclusively.

Whole-cortex networks

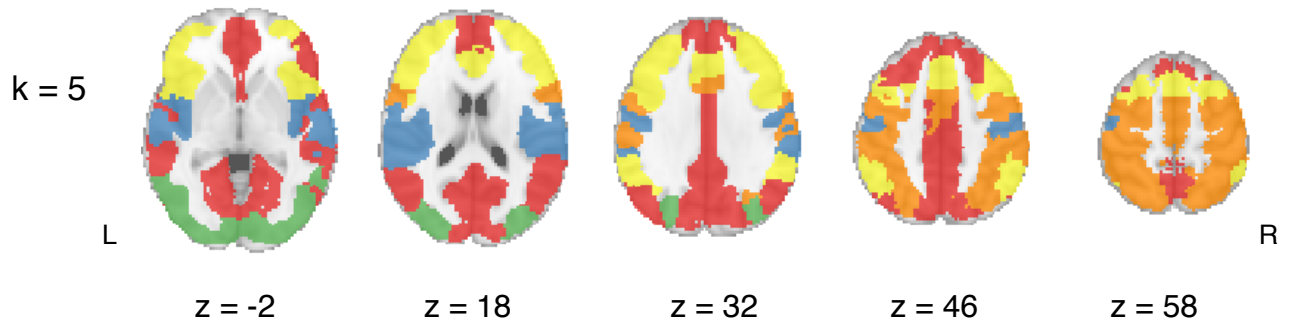


Figure 3. Co-activation based hierarchical clustering of the entire cluster reveals large-scale functional networks. We clustered cortex using a 30% Harvard-Oxford grey matter mask on the basis of individual voxels' co-activation with the rest of the brain. The solution with 5 clusters reveals commonly identified networks, such as the default network (red), visual network (green), dorsal attention network (orange), a auditory / motor network (blue), and the task-positive network (yellow). Subsequent analyses focus on the task-positive network as it includes various regions that have all been associated with goal-oriented cognition.

Because structure-to-function mappings can be identified at multiple spatial scales, we iteratively extracted 2- through 30-cluster flat cluster solutions within the task-positive network (Figure 4) and assessed their validity using the silhouette score—a commonly used measure of inter-cluster coherence. As selecting the correct number of regions is an difficult, if intractable, problem, we used the silhouette score to reject poor solutions, rather than to argue that the particular number of regions chosen hold neuro-scientific meaning. Silhouette scores reached local maxima at 3, 9, 15 and 27 regions (Figure 4A). We primarily focus on the first three solutions as they provide insight into the organization of frontal cortex at spatial scales relevant to fMRI research, but make available the images for more fine-grained solutions available in Appendix II. Moreover, we chose to focus on regions in lateral frontal cortex. As such, we only

name and analyze regions outside of lateral frontal cortex at the coarsest level of granularity in which they split from clusters including lateral frontal cortex; for example, lateral parietal cortex (LPar) separates from the fronto-parietal network in the nine-cluster solution; thus, its subdivisions present in the fifteen-cluster solution are not discussed further.

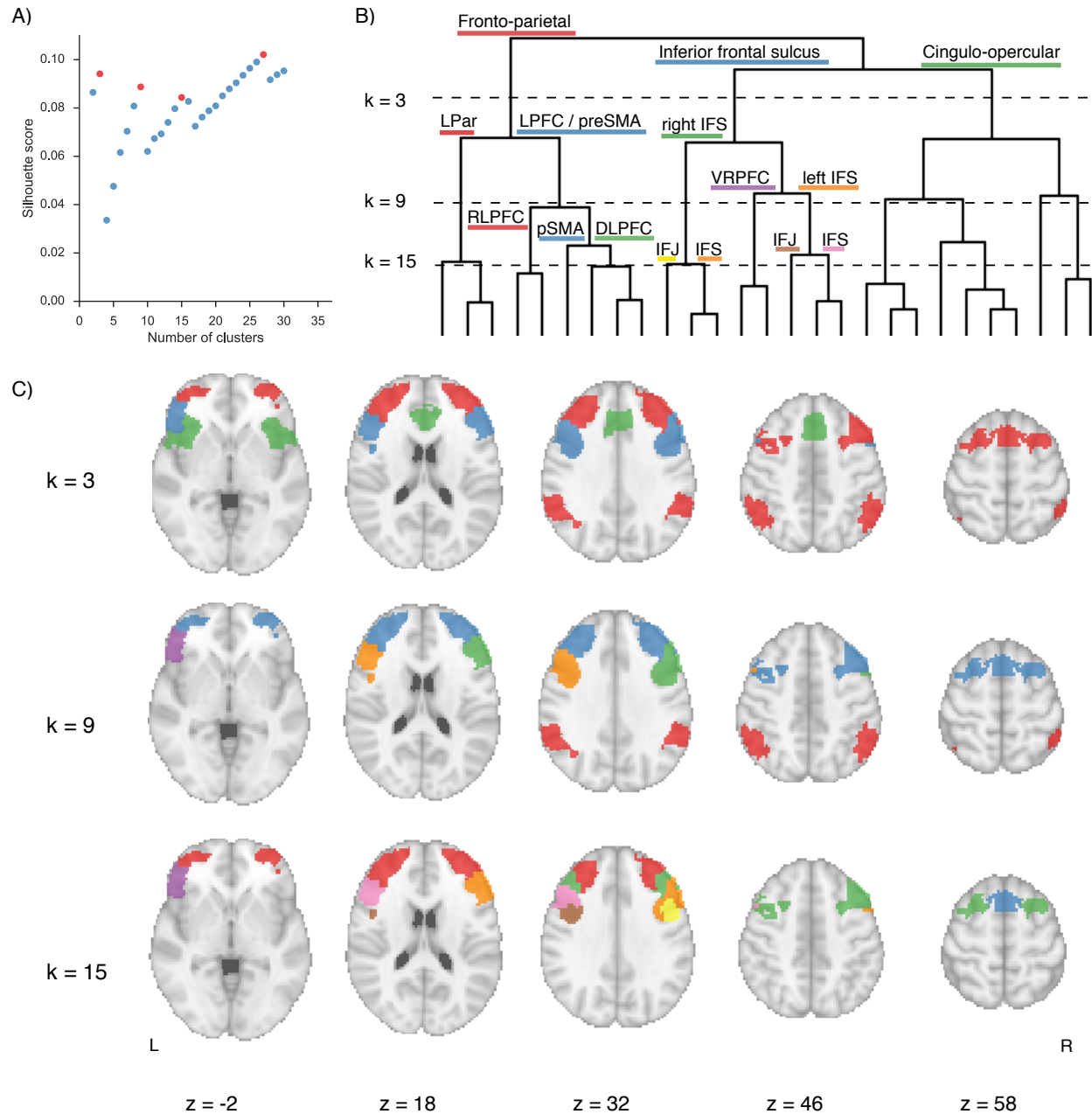


Figure 4. Co-activation based clustering of task-positive network. A) Silhouette scores assess the

consistency of clusters relatively to data they were derived from. Silhouette scores reached local maxima (in red) at 3, 9, 15 and 27 regions for the task-positive network. B) Dendrogram of hierarchical clustering. The task positive network is composed fronto-parietal, cingulo-opercular and an inferior frontal sulcus sub-networks that further fractionate into smaller regions. Subjective names were given with assistance from the Harvard-Oxford atlas and colors were assigned at each spatial scale. To focus on lateral frontal regions, clusters that were entirely out of the lateral frontal cortex were not examined or named in more detail (e.g. cingulo-opercular network at $k=3$, lateral parietal cortex at $k=9$). C) Spatial images of solutions at 3, 9, and 15 regions. Colors of regions correspond colors assigned in dendrogram. LPar: lateral parietal cortex; LPFC: lateral prefrontal cortex; IFS: inferior frontal sulcus; IFJ: inferior frontal junction; preSMA: pre-supplementary motor area; DLPFC: dorsolateral prefrontal cortex; RLPFC: rostralateral prefrontal cortex; VRPFC: ventrorostral prefrontal cortex.

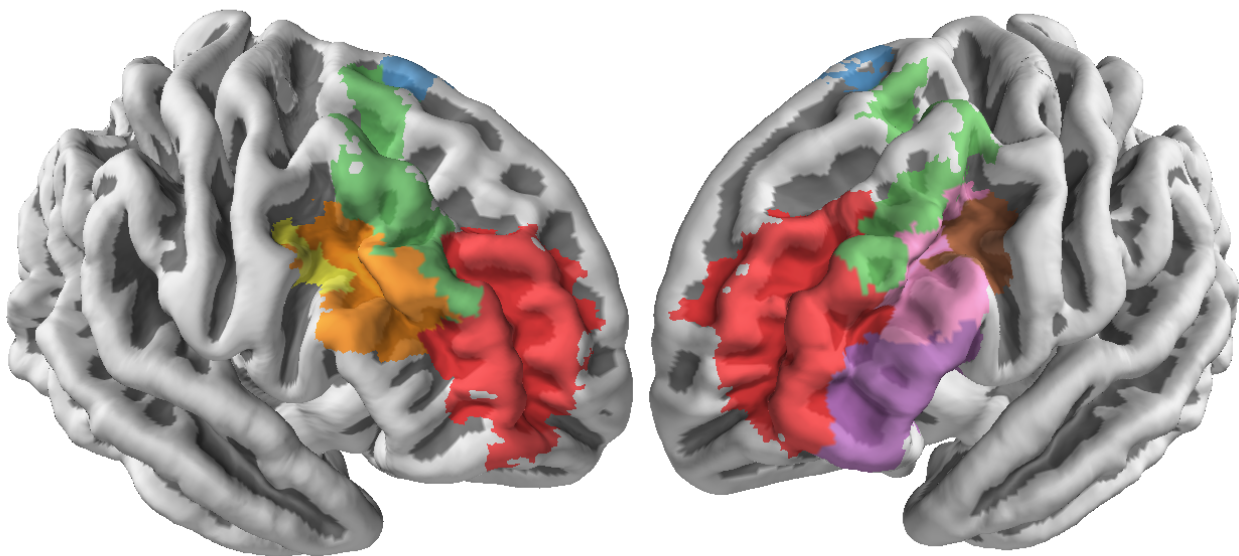


Figure 5. Lateral frontal clusters of task-positive network for the 15-cluster solution mapped onto pial brain surface. Colors match those use din Figure 4.

Anatomical correspondence of lateral frontal task-positive clusters

To better understand the anatomical location of our clusters, we compared them to previously defined sub-regions from a probabilistic structural atlas (Harvard-Oxford) and cytoarchitecture {Petrides:2005hc}. The task-positive network first fractionated into three sub-networks consistent networks previously derived using resting-state fMRI: the fronto-parietal cognitive control network, the inferior frontal sulcus and the cingulo-opercular network (Figure 4C). The fronto-parietal network bilaterally spanned anterior and middle portions of the middle frontal gyrus, and a small posterior portion of the superior frontal gyrus. This network mapped onto dorsal medial frontal cortex into a location consistent with definitions of pre-SMA as well as lateral portions of parietal cortex. The inferior frontal cluster included the entirety of the inferior frontal sulcus bilaterally, spanning from its most posterior aspect adjacent to the pre-central sulcus to its most anterior aspect near the frontal pole. This cluster included ventral portions of middle frontal gyrus as well as dorsal portions of inferior frontal sulcus near area 9/46. Additionally, this cluster also included inferior frontal gyrus pars triangularis as well as posterior aspects of lateral frontal pole, but only in the left hemisphere. Finally, the cingulo-opercular network cluster spanned portions of midcingulate cortex (MCC) previously associated with cognitive control as well as anterior aspects of the operculum and insula. This cluster extended dorsally as far as inferior frontal gyrus, pars opercularis in the right hemisphere, but only to a small extent. Notably, portions of the superior frontal gyrus corresponding to area 9 were absent from any of these networks.

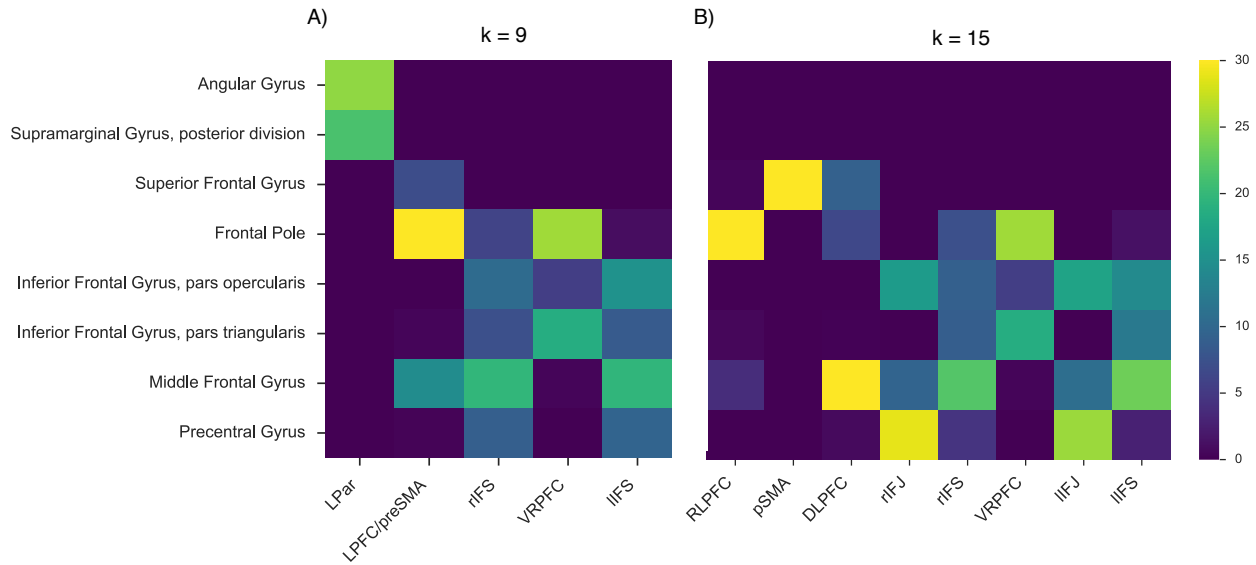


Figure 5. Location of clusters according to the Harvard-Oxford anatomical atlas for the 9 (A) and 15 (B) cluster solution. Probability of occurring in each Harvard-Oxford region was calculated for all clusters and regions with greater than average 3% probability across all clusters are shown. Only clusters labeled Figure 4B are shown for brevity. Color scale is truncated at 30% to maximize visual differences.

The fronto-parietal network fractionates into two clusters in the nine-cluster solution: a frontal cluster --- including lateral prefrontal cortex and pre-SMA --- and a lateral parietal cluster. The lateral parietal cluster spans portions of both the angular and posterior supramarginal gyri. The frontal cluster further fractionates into three bilateral clusters in the fifteen-cluster solution: pre-SMA, dorsolateral PFC (DLPFC), and rostralateral PFC (RLPFC). The pre-SMA cluster is located on the dorsomedial aspects of superior frontal gyrus, extending slightly onto lateral aspects of superior frontal gyrus (this and nearby regions are discussed in more detail in Chapter 1). DLPFC is located primarily in the middle frontal gyrus, spanning its entire length from precentral gyrus on the caudal end and lateral frontal pole (BA10) on the rostral end. The middle portion of this DLPFC cluster is consistent with cytoarchitectonic definitions of BA 9/46 as this

region is located squarely in middle frontal gyrus; notably, this cluster is primarily located in dorsal and middle portions of the gyrus near the intermediate frontal sulcus, with no voxels near the inferior frontal sulcus. Finally, RLPFC is located entirely within lateral frontal pole, adjacent to DLPFC caudally; RLPFC spans BA10, and abuts rostral portions of area 46 and 9/46 in middle frontal gyrus.

The inferior frontal sulcus network fractionates into three unilateral clusters in the nine-cluster solution: right and left inferior sulcus (IFS) and a left ventrorostral PFC (VRPFC). On both hemispheres, IFS spans the entire sulcus, abutting the precentral sulcus at its caudal end and lateral frontal pole (RLPFC) on its rostral end. In both cases, IFS includes the ventral bank of middle frontal gyrus-- inferior to the intermedial frontal sulcus-- and dorsal inferior frontal gyrus. Further ventroanterior in the left hemisphere, VRPFC spanned both inferior frontal gyrus pars-triangularis, orbitalis and ventro-lateral aspects of frontal pole, consistent with descriptions of BA 47/12. In the fifteen-cluster solution, both right and left IFS further fractionate into a caudal inferior frontal junction (IFJ) region and a mid-IFS region. The contralateral homologues show a high degree of similarity. The IFJ cluster is located at the most posterior end of the inferior frontal sulcus, spanning precentral, inferior frontal and middle frontal gyri. The cluster is mostly buried in the fundus of the sulci and is consistent with previous reports of an IFJ region (e.g. MNI coordinates 48, 4, 33; {Brass:2005iw}{MuhleKarbe:2015kf}). Immediately rostral to IFJ is the remainder of the IFS cluster, which spans both middle and inferior frontal gyri; as such the portions of this cluster in middle frontal gyrus are consistent with area 9/46v {Petrides:2005hc}.

In summary, we identified spatially distinct clusters across lateral frontal cortex at various level of granularity that composed a distributed task-positive network. Although these co-activation based clusters map onto previously identified anatomical boundaries and

hypothesized functional regions, they only showed moderate correspondence with cyto-architectonic areas and individual regions spanned gross morphological features (e.g. ‘IFS’ encompassed both ventral middle frontal gyrus and dorsal inferior frontal gyrus). Next, to provide direct insight into the functions of the clusters we identified, we applied two approaches. First, we determined which other brain regions co-activate with each cluster, in order to reveal their functional networks. Second, we probed semantic metadata from Neurosynth to determine which psychological states predict the activation of each cluster.

Distinct patterns of whole-brain co-activation of frontal clusters of the task-positive network

We directly contrasted the whole-brain co-activation patterns of the lateral frontal clusters at two scales to better understand the functional networks that each region participated with. Since all the clusters we identified belonged to the same “task-positive” network, their overall co-activation patterns were relatively similar; thus we explicitly sought to determine voxels across the brain that differentially co-activated with clusters in lateral frontal cortex.

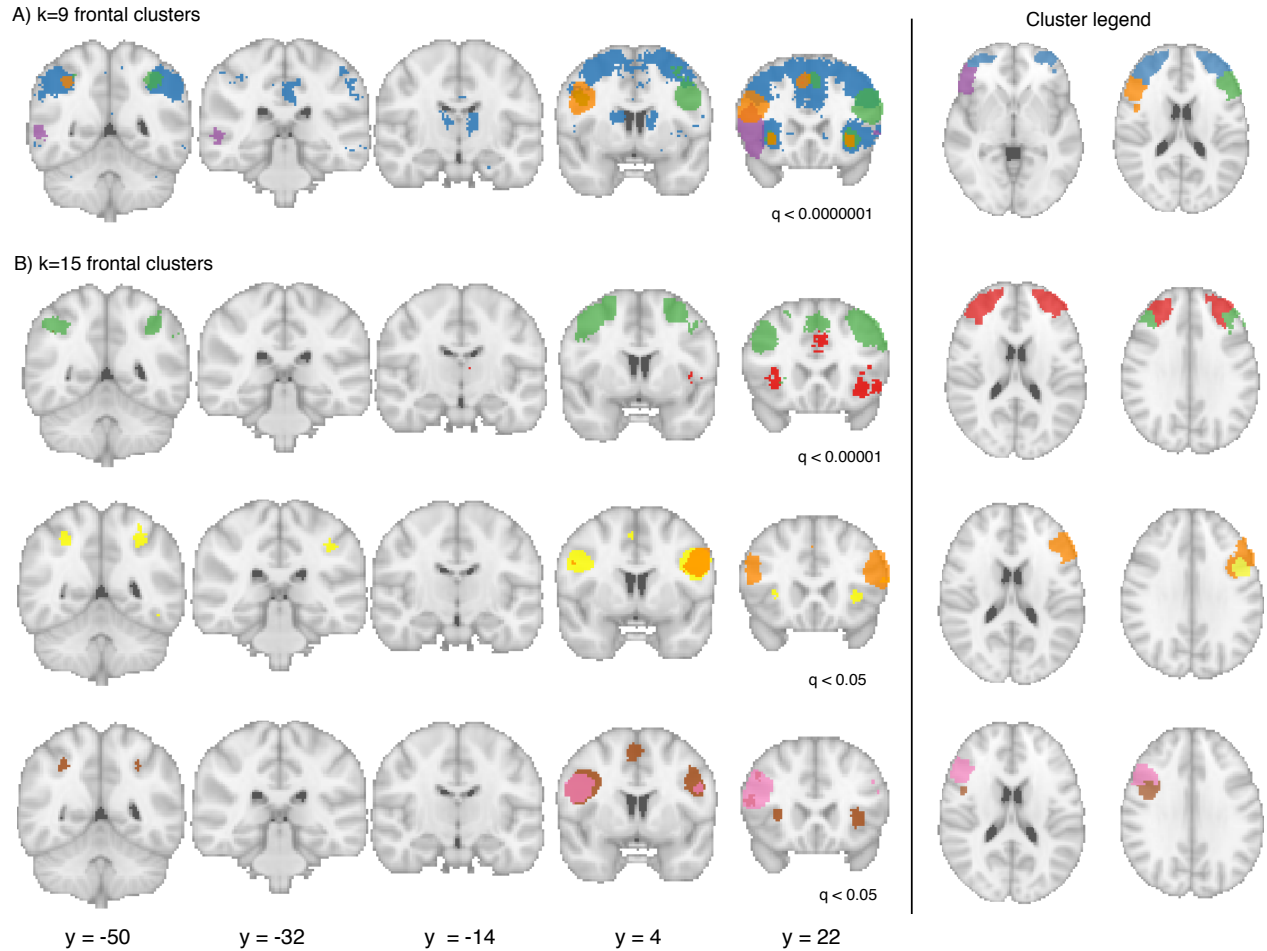


Figure 6. Meta-analytic co-activation contrasts for lateral frontal clusters in the (A) nine-cluster and B) fifteen-cluster solution. Colored voxels indicate significantly greater co-activation with the seed region of the same color (at right) than control regions in the same row. Images are presented using neurological convention and were whole-brain corrected using a false discovery rate (FDR); multiple correction threshold (q) was adjusted for each comparison to avoid overcrowding as is indicated below each. Major subcortical structures are labeled.

In the nine-cluster solution, we contrasted the co-activation of four frontal clusters: LPFC/pre-SMA, right and left IFS and VRPFC (Figure 6). Consistent with these clusters' membership in the task-positive network, differences in whole co-activation were relatively subtle. In parietal cortex, LPFC/pre-SMA showed greater co-activation with the outer surface of

inferior parietal lobule –particularly in angular gyrus— whereas both IFS clusters co-activated more strongly with cortex in the intraparietal sulcus, on their respective hemispheres. In contrast, left VRPFC showed greater co-activation with a left posterior middle temporal gyrus, a region previously associated with language and object recognition. Further anterior, LPFC/pre-SMA showed greater co-activation with mid-cingulate cortex —posterior and anterior— and pre-SMA. However, IFS also co-activated with pre-SMA, highlighting that IFS and LPFC/pre-SMA show moderate amounts of co-activation across tasks. These three regions also showed robust co-activation with anterior insula, which has been implicated in goal-oriented cognition. Subcortically, LPFC/pre-SMA showed greater co-activation with both the thalamus and dorsal striatum, consistent with the critical role of cortico-striatal loops in the regulation of information to lateral prefrontal cortex {Hazy:2007gm, Frank:2011kl}.

At the more fine-grained scale of fifteen task-positive clusters, we contrasted the co-activation of the six clusters located in lateral frontal cortex. To highlight the subtle differences in co-activation between the newly formed clusters, we contrasted the co-activation of related clusters that combined to form a single cluster in the nine-cluster solution: RLPFC and DLPFC, left IFJ and IFS, and right IFJ and IFS. (Figure 6B). DLPFC showed greater co-activation than RLPFC with lateral parietal cortex bilaterally, focused near the intraparietal sulcus, whereas RLPFC showed greater co-activation with a more rostral portion of lateral parietal cortex, in supramarginal gyrus (not pictured). On the medial surface, RLPFC showed greater co-activation with midcingulate cortex (posterior and anterior), whereas DLPFC showed greater co-activation with more dorsal aspects of MCC and pre-SMA. RLPFC showed much greater co-activation with the anterior insula – notable due to the important role this region is thought to play in goal-directed cognition. Subcortically, RLPFC showed a small portion of stronger co-activation with

the thalamus, important given the important role of the thalamus in broadcasting information throughout the brain. There were relatively fewer differences between IFJ and IFS. In both hemispheres, IFJ showed greater co-activation with other ‘task-positive’ regions, such as the intraparietal sulcus, SMA and the anterior insula. In sum, the co-activation patterns of frontal task-positive clusters demonstrate these regions participate with somewhat different regions across the brain, although the extent of these differences vary across lateral frontal cortex.

Meta-analytic functional preference profiles

Next, we used a data-driven approach that surveyed a broad range of psychological states to determine if clusters in the task-positive network are differentially recruited by psychological states. For each cluster, we trained a multivariate classifier to predict which studies activated the cluster using a set of 60 psychological topics derived by applying a standard topic modeling approach to the abstracts of articles in the database (Poldrack et al., 2012b) (Table 1). From the resulting fitted classifiers, we calculated the extent to which each topic predicted activity in each cluster and restricted interpretation to significant associations using permutation testing (False Discovery Rate $q < 0.01$). To highlight differences at various spatial scales, we begin by comparing the functional profiles of the three task-positive sub-networks, and then further interrogate the differences between their constituent regions at finer scales.

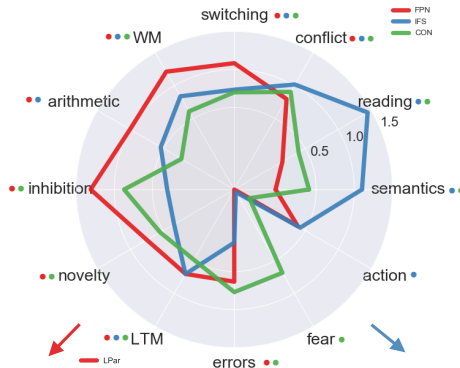
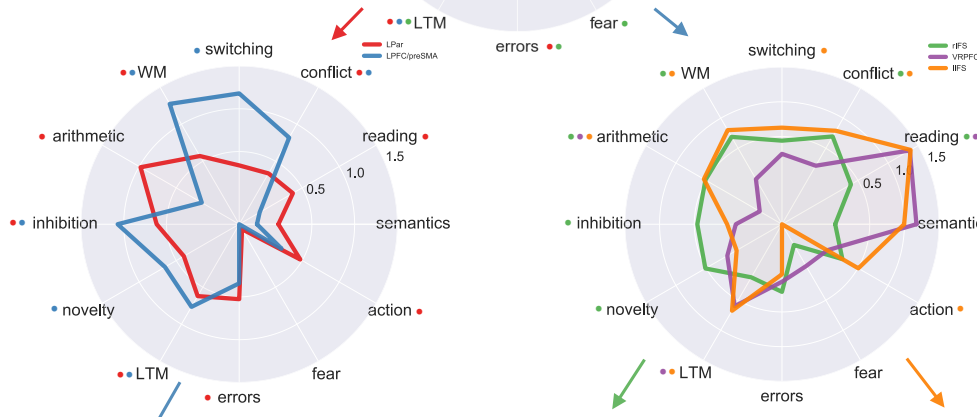
A) $k = 3$ B) $k = 9$ C) $k = 15$ 

Figure 7. Functional preference profile of task-positive network clusters. A) Fronto-parietal network (FPN), inferior frontal sulcus (IFS) and cingulo-opercular network (CON) showed distinct functional signatures. B & C) We examined finer-grained functional shifts the fronto-parietal (FPN) and inferior frontal networks at two finer spatial scales—9 and 15 TPN clusters—comparing regions in accordance with the structure denoted by the hierarchical dendrogram. Colored arrows denote which clusters from coarser solutions are being examined in more detail. Strength of associations is measured in log odds-ratio, and permutation-based significance (False

Discovery Rate $q < 0.01$) is indicated next to each psychological concept by color-coded dots corresponding to each region.

Task-positive sub-networks

We observed dissociable, yet overlapping, functional signatures between the three task-positive sub-networks, consistent with their relatively late merge into a network in the hierarchical clustering dendrogram (Figure 7A). The fronto-parietal network (FPN) showed a strong preference for cognitive control processes, including working-memory, conflict, switching, and inhibition. Moreover, the FPN was also preferentially recruited by states that indicate the need for additional cognitive control – error and novelty detection -- and require mental operations (i.e. arithmetic). Although the FPN was robustly associated with all cognitive control related processes, consistent with a role in effortful, goal-directed cognition, both the CON and IFS were recruited for certain cognitive control processes. Notably, conflict and long-term memory recruited all three networks to a similar extent. Moreover, working-memory and switching also significantly, but to a lesser extent than FPN, recruited the IFS and CON. The CON was additionally recruited by inhibition, novelty and error detection, consistent with theories suggesting CON activity is not simply arousal or salience related, a may operate as a ‘control’ network in the brain {Power:2013kk}. Our results suggest that cognitive control processes that are generally thought to be the provenance of the FPN rely on a distributed set of regions throughout the task-positive network. In addition, the CON was the only task-positive regions recruited by affect (i.e. fear), consistent previous evidence linking midcingulate cortex with negative affect. Finally, the IFS was characterized by a strong recruitment by language processes (i.e. reading, speech, semantics), consistent with a well established role of ventro-lateral PFC in language.

Fronto-parietal network sub-regions

Upon closer inspection, we observed that constituent regions of the FPN showed substantially different functional profiles. First, in the nine-region solution (Figure 7B), LPFC/pre-SMA, was more strongly associated with a variety of cognitive control processes critical for flexible behavior (e.g. conflict, working-memory, switching) whereas LPar was more strongly associated with ‘automatable’ processes (e.g. reading, arithmetic) and lower-level sensory and motor function that may support higher level processing (e.g. action, visual-spatial, sensory). Although this dissociation supports most existing cognitive control models, it was notable that LPar was significantly associated (although to a lesser extent than frontal regions) with a wide-range of cognitive control processes, suggesting the interaction between parietal and frontal regions is critical for goal-directed cognition.

Next, in the fifteen-region solution, we compared the functional profiles of the frontal regions that composed LPFC/pre-SMA, and observed appreciable differences between them even at this more fine-grained scope. Pre-SMA showed a distinct profile from the two lateral clusters, showing a weaker but significant, association with core cognitive control processes such as switching, conflict, and WM. Moreover, pre-SMA was more strongly associated with motor function, language and arithmetic processing. In contrast, both lateral PFC clusters were strongly associated with a variety cognitive control processes, including switching, conflict, WM, inhibition and novelty detection. However, these lateral PFC clusters were functional dissociable: DLPFC was more strongly recruited by working memory, while RLPFC was more strongly recruited by inhibition and novelty detection. Finally, all three clusters —particularly lateral ones— were significantly recruited by LTM, suggesting this process requires a distributed set of regions through the task-positive network.

Inferior frontal sulcus sub-regions

We next analyzed the functional profiles of sub-regions of the IFS network: right and left IFS and VRPFC (Figure 7B). The most striking functional difference we observed between inferior frontal task-positive regions was a strong left-lateralized preference for LTM and language (e.g. reading, semantics, and speech) in both the ventro-rostral PFC and left inferior frontal sulcus, consistent with the long held belief that language is left lateralized in most individuals. However, right IFS also showed a significant-- although much weaker-- association with reading, suggesting language is not entirely left-lateralized.

Comparing the two IFS contralateral homologues revealed relatively small differences with respect to their association with cognitive control processes. In particular, both clusters were similarly moderately recruited by WM and conflict, and lIFS was associated by a marginally greater extent with switching. However, rIFS was the only cluster in this network recruited by novelty and inhibition, the latter consistent with previously documented right lateralization of inhibition in VLPFC. However, as a whole, we observed much less specialization to specific cognitive control processes between IFS regions in contrast to sub-regions of the FPN. Finally, left IFS was the only frontal region across the task-positive network significantly associated with ‘action’ – a topic representing high-level motor planning— suggesting this region may be important for linking high-level goals with motor function.

Taking a closer look at the two IFS contralateral clusters (Figure 7C), revealed surprisingly few differences between IFS and the more posterior IFJ. Across both hemispheres, the only notable difference we observed was that only rIFS, and not rIFJ, was significantly associated with novelty and inhibition. Thus, although the co-activation of these clusters was

sufficiently different to separate them into two clusters, their functional profiles suggest they may be involved in similar psychological domains.

Functional similarity across clusters

To more quantitatively examine the similarity between the sub-regions we identified, we calculated the Pearson correlation distance between each pair of frontal clusters in fifteen-cluster solution on the basis of their complete functional profile across the 60 topics (Figure 8). This analysis confirmed our qualitative assessments as --within each hemisphere-- IFS and IFJ showed the lowest functional distance of any pair (Pearson distance for left hemisphere: 0.07, right hemisphere: 0.18). However, IFS and IFJ were not simply functionally vague, as the greatest functional difference we observed was between RLPFC and IIFJ (0.82). Notably, the second most similar pair was pre-SMA and rIFS (1.7). The high base rate of activity in both IFS and pre-SMA, as well as their moderate association with many cognitive control processes, it's possible that both of these regions play non-specific, domain-general roles in goal-directed cognition. Moreover, the high similarity between IFS and pre-SMA despite being in different 'networks', suggests the functional differences between regions is constrained, but not strictly dictated, by co-activation differences.

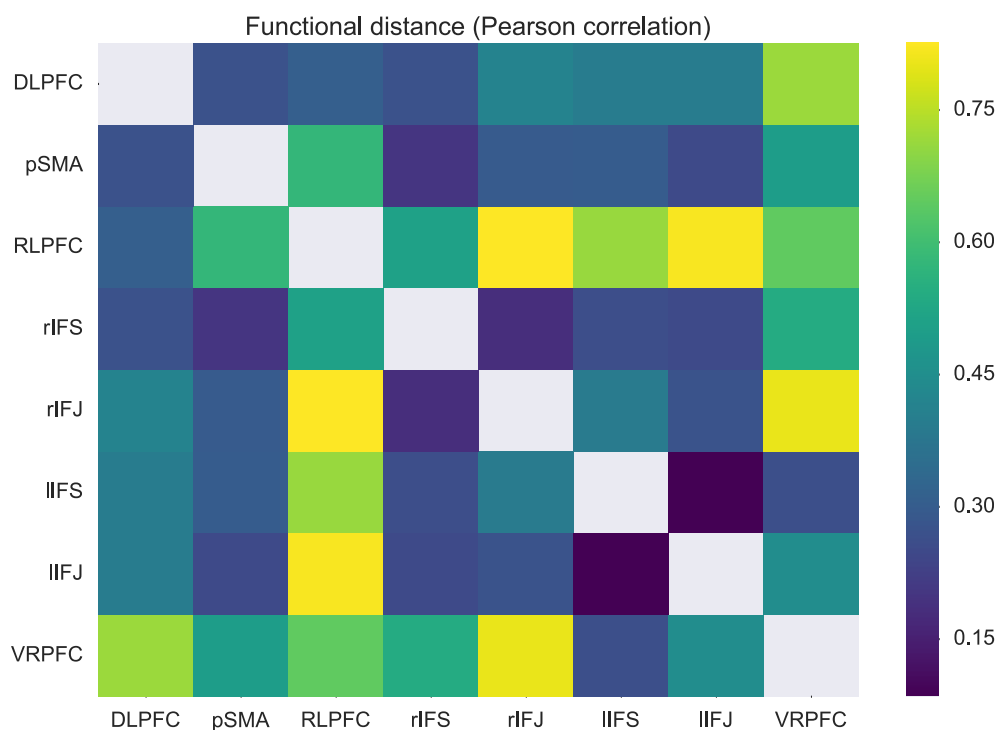


Figure 8. Pairwise correlation distance of functional profiles between frontal regions in the fifteen-region solution. Note the similarity function IFJ and IFS within each hemisphere.

Topic name	Top loading words
action	action actions motor goal mirror planning imitation execution directed
arithmetic	number numerical arithmetic numbers digit calculation mental symbolic distance
conflict	conflict interference incongruent stroop congruent selection competition color reaction
errors	error errors monitoring correct feedback creative creativity driving incorrect
fear	fear anxiety threat conditioning cs extinction conditioned aversive phobia
inhibition	inhibition inhibitory stop motor sustained nogo transient suppression inhibit
LTM	memory retrieval encoding recognition episodic items recall words memories
novelty	target targets novelty oddball distractor distractors deception mismatch identity
reading	reading sentences language comprehension sentence word syntactic phonological chinese
semantics	semantic words word lexical verbs abstract meaning verb nouns retrieval
switching	switching rule executive switch rules flexibility shifting aggression shift
WM	memory working wm load verbal maintenance delay encoding capacity

Table 1. Topics most strongly associated with task-positive regions used in Figure 6. Nine strongest loading words for each topic are listed, in descending order of association strength.

Discussion

Discussion points:

- Cognitive control processes are more distributed than some would expect, and definitely implicate the cingulo-opercular network
- Fit to existing models:
 - Rostro-caudal axis
 - Possibly, when comparing DLPFC to RLPFC. However, many cognitive control functions are distributed, which is in contrast to theory. In particular, memory is hypothesized to show a hierarchical order, and it is among the most distribution of fuctions
 - IFJ and set switching?
 - While our results suggest that IFJ is indeed involved in set-switching and cognitive control more than some people have claimed, other regions in the FPN are much more robustly associated with switching, suggesting this may not be IFJ's primary role
 - IFJ has very high activation rate, so it is likely to being doing something fundamental that underlies many tasks
 - IIFJ was involved with 'action'. As such, it may be that rIFJ is indeed a link between high-level representations in dLPFC and motor regions.